11176 *Inorg. Chem.* **2009**, *48*, 11176–11186
DOI: 10.1021/ic901519s

Inorganic Chemistry
Article

Synthesis, Structure, and Photophysical Characterization of Blue-Green Luminescent Zinc Complexes Containing 2-Iminophenanthropyrrolyl Ligands

Clara S. B. Gomes,[†] Pedro T. Gomes,*[,†] M. Teresa Duarte,[†] Roberto E. Di Paolo,[†] António L. Maçanita,[†] and Maria José Calhorda[‡]

[†]*Centro de Química Estrutural, Departamento de Engenharia Química e Biológica, Instituto Superior Técnico, Av. Rovisco Pais, 1049-001 Lisboa, Portugal, and* [‡]*Departamento de Química e Bioquímica, Faculdade de Ciências, Universidade de Lisboa, 1749-016 Lisboa, Portugal*

Received July 30, 2009

New 2-iminophenanthro[9,10-*c*]pyrrole ligand precursors containing phenyl or 2,6-diisopropylphenyl groups at the imine nitrogen substituent, 2-arylformiminophenanthro[9,10-*c*]pyrroles (aryl = phenyl **IIa**, 2,6-diisopropylphenyl **IIb**) were synthesized and deprotonated *in situ* with NaH, originating solutions of the corresponding sodium salts (**IVa**, **IVb**). The reaction of these salts with zinc chloride gave the homoleptic bis-ligand Zn(II) complexes [Zn(κ^2*N*,*N*′-2-arylformiminophenanthro[9,10-*c*]pyrrolyl)$_2$] (aryl = phenyl **2a**, 2,6-diisopropylphenyl **2b**). The new ligand precursors and complexes were characterized by NMR, elemental analysis, UV/vis spectroscopy, and X-ray crystallography, when possible. The photophysical characterization was carried out using steady-state and picosecond time-resolved luminescence techniques in solution. The influence of the π-extended conjugation of the condensed phenanthro group on the deprotonated iminopyrrolyl ligands coordinated to Zn^{2+} greatly enhances fluorescence quantum yields of the complexes (**2a**, **2b**) in relation to those of their ligand precursors (**IIa**, **IIb**). Complex **2a** shows emission in the green spectral region (λ_{max} = 494 nm), presenting the highest fluorescence quantum yield (ϕ_f = 8.8%). In the case of the complex **2b** (ϕ_f=3.9%), the bulkiness of the 2,6-diisopropyl substituents of the arylimino group highly restricts the aryl ring rotation toward coplanarity with the ligand framework, inducing a shift in the emission to the blue region (λ_{max} = 459 nm). The values of the radiative (k_f) and radiationless rate constants (k_{nr}) show that the fluorescence quantum yield enhancement in the complexes results from a 50-fold increase in k_f values, indicating much more allowed $\pi-\pi^*$ transitions in complexes **2a** and **2b** than those occurring in the ligand precursors **IIa** and **IIb**, with an essentially $n-\pi^*$ character. These assignments were confirmed by density-functional theory (DFT) and time-dependent DFT (TD-DFT) molecular orbital calculations. Simple 2-aryliminopyrrole ligand precursors (**Ia**, **Ib**) and their Zn(II) complexes (**1a**, **1b**) were also prepared to compare their photophysical properties with those of the corresponding 2-aryliminophenanthro-[9,10-*c*]pyrrolyl compounds.

Introduction

In recent years, great interest in the synthesis of coordination and organometallic compounds with luminescent properties has emerged, mainly for use in display technology, because of their potential applications in LEDs (Light-Emitting Diodes).[1−3] These compounds contain chromophores that emit visible light at wavelengths depending on the composition and structure of the material. Research in this area has the purpose of obtaining red, green, and blue emissive materials, to be used together and be able to produce the full color spectrum and white emitters for the use in lighting applications.[4] In 1963, Pope reported the first example of electroluminescence observed in an organic semiconductor, a single crystal of anthracene.[5] Despite this publication, the commercial value of this discovery was only realized in 1987 when Tang and VanSlyke, from Eastman Kodak, reported the observation of electroluminescence in aluminum tris(quinoline-8-olate), Alq_3, an organic thin-film device prepared by vapor deposition.[6] Several approaches have been described to build full color displays, and this area

*To whom correspondence should be addressed. E-mail: pedro.t.gomes@ist.utl.pt. Phone: +351 218419612. Fax: +351 218419612.

(1) Holder, E.; Langeveld, B. M. W.; Schubert, U. S. *Adv. Mater.* **2005**, *17*, 1109–1121.
(2) Evans, R. C.; Douglas, P.; Winscom, C. J. *Coord. Chem. Rev.* **2006**, *250*, 2093–2126.
(3) Geffroy, B.; le Roy, P.; Prat, C. *Polym. Int.* **2006**, *55*, 572–582.
(4) Borchardt, J. K. *Mater. Today* **2004**, *7*, 42–46.
(5) Pope, M.; Kallmann, H. P.; Magnante, P. *J. Chem. Phys.* **1963**, *38*, 2042–2043.
(6) Tang, C. W.; VanSlyke, S. A. *Appl. Phys. Lett.* **1987**, *51*, 913–915.
(7) For example: (a) Lamansky, S.; Djurovich, P.; Murphy, D.; Abdel-Razzaq, F.; Lee, H.-E.; Adachi, C.; Burrows, P. E.; Forrest, S. R.; Thompson, M. E. *J. Am. Chem. Soc.* **2001**, *123*, 4304–4312. (b) Pandya, S.; Yu, J.; Parker, D. *Dalton Trans.* **2006**, 2757–2766. (c) Wang, S. *Coord. Chem. Rev.* **2001**, *215*, 79–98.

 Published on Web 10/28/2009

Chart 1. Homoleptic Bis(aryliminopyrrolyl) Metal Complexes: Square Planar **A** (M = Ni; R = R^2 = H; R^1 = ^{i}Pr.[15,18] M = Ni; R = R^1 = R^2 = Me.[17] M = Ni; R = R^2 = H; R^1 = Me.[18] M = Co; R = Me; R^1 = ^{i}Pr, R^2 = H[16a]) and tetrahedral **B** (M = Co; R = H; R^1 = ^{i}Pr.[16a] M = Co; R = H, Me; R^1 = H, Me.[16a] M = Zn; R = H; R^1 = ^{i}Pr[19])

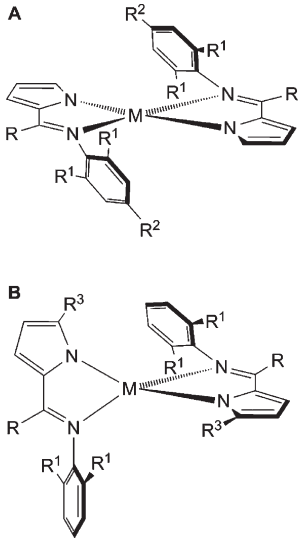

of investigation was rapidly extended to a wide range of metal complexes, which include for example, Ir(III),[7a] lanthanides such as Eu(III) and Tb(III),[7b] but also Al(III), Zn(II), and B(III)[7c] among others. In fact, luminescent Zn(II) complexes containing chelating ligands, such as benzothiazolates,[8a] quinolinolates,[8b] salicylaldiminates,[8c] dipyridylamino,[7c] 7-azaindolyl,[7c] 2-(2-pyridyl)indolyl,[7c] and anilido-imine,[9] have been widely studied in recent years, not only for their use in LEDs but also for application in imaging techniques[10] and as fluorescent sensors for Zn^{2+} in biological systems.[11]

Iminopyrrolyl bidentate chelating ligands, which contain pyrrolyl anionic ring and neutral imine donor moieties, may be considered structurally similar to salicylaldiminate, anilido-imine or 2-(2-pyridyl)indolyl ligands and have been employed in the synthesis of several transition-metal compounds.[12] The first syntheses of homoleptic metal complexes of Co(II), Ni(II), Pd(II), Cu(II), and Zn(II) containing these kind of ligands, although only with alkylimino groups, were reported in the 1960s.[13] More recently, these ligands have been employed in the syntheses of metal complexes that behave as precatalysts for olefin polymerization.[14]

We have been interested in the chemistry of iminopyrrolyl ligands, and recently our group and other authors have reported the synthesis and characterization of several homoleptic square planar or tetrahedral complexes containing arylimino derivatives of these ligands with metals such as Co(II),[15,16] Ni(II),[15,17,18] and Zn(II)[19] (Chart 1).

The closed-shell electronic configuration of the latter ion (d^{10}) turns Zn(II) by itself spectroscopically inactive, and thus the luminescent properties of its complexes can be tuned by the modification of the corresponding ligands.[9] In this paper, we report the synthesis of [Zn(2-aryliminopyrrolyl)$_2$] containing simple iminopyrrolyl ligands, such as those represented in Chart 1 (aryl = Ph; 2,6-^{i}Pr$_2$Ph), and the characterization of their absorption and emission properties. We further describe the modification of the pyrrolyl ligand backbone, to improve its chromophore properties, by the addition of a fused aromatic ring system, such as phenanthrene, to the pyrrole C3−C4 bond, allowing the synthesis of new 2-iminophenanthropyrrolyl ligand precursors. Subsequently, we describe the synthesis and molecular characterization of new [Zn(2-aryliminophenanthro[9,10-*c*]pyrrolyl)$_2$] and compare their luminescence features with those of the corresponding simple [Zn(2-aryliminopyrrolyl)$_2$]. We have characterized the photophysical properties of these compounds using steady-state and time-resolved luminescence techniques in solution. Density-functional theory (DFT) and time-dependent DFT (TD-DFT) calculations (ADF program) were also carried out for these new ligand precursors and for their Zn(II) complexes to assign the electronic transitions, to determine the geometry of the first excited state, and to try to rationalize the luminescence behavior exhibited.

Experimental Section

General Procedures. All experiments dealing with air- and/or moisture-sensitive materials were carried out under inert atmosphere using a dual vacuum/nitrogen line and standard Schlenk techniques. Nitrogen gas was supplied in cylinders by specialized companies (e.g., Air Liquide, etc.) and purified by passage through 4 Å molecular sieves. Unless otherwise stated, all reagents were purchased from commercial suppliers (e.g., Acrös, Aldrich, Fluka) and used without further purification. All solvents to be used under inert atmosphere were thoroughly deoxygenated and dehydrated before use. They were dried and purified by refluxing over a suitable drying agent followed by distillation under nitrogen. The following drying agents were used: sodium (for toluene, diethyl ether, and tetrahydrofuran (THF)), calcium hydride (for hexane and dichloromethane). Deuterated solvents were dried by storage over 4 Å molecular

(8) For example: (a) Yu, G.; Yin, S.; Liu, Y.; Shuai, Z.; Zhu, D. *J. Am. Chem. Soc.* **2003**, *125*, 14816–14824. (b) Ghedini, M.; La Deda, M.; Aiello, I.; Grisolia, A. *Inorg. Chim. Acta* **2004**, *357*, 33–40. (c) Chang, K.-H.; Huang, C.-C.; Liu, Y.-H.; Hu, Y.-H.; Chou, P.-T.; Lin, Y.-C. *Dalton Trans.* **2004**, 1731–1738.

(9) Su, Q.; Gao, W.; Wu, Q.-L.; Ye, L.; Li, G.-H.; Mu, Y. *Eur. J. Inorg. Chem.* **2007**, 4168–4175.

(10) (a) Pascu, S. I.; Waghorn, P. A.; Conry, T. D.; Betts, H. M.; Dilworth, J. R.; Churchill, G. C.; Pokrovska, T.; Christlieb, M.; Aigbirhio, F. I.; Warren, J. E. *Dalton Trans.* **2007**, 4988–4997. (b) Descalzo, A. B.; Xu, H.-J.; Xue, Z.-L.; Hoffmann, K.; Shen, Z.; Weller, M. G.; You, X.-Z.; Rurack, K. *Org. Lett.* **2008**, *10*, 1581–1584.

(11) (a) Béreau, V. *Inorg. Chem. Commun.* **2004**, *7*, 829–833. (b) Wu, Z.; Chen, Q.; Yang, G.; Xiao, C.; Liu, J.; Yang, S.; Ma, J. S. *Sens. Actuators, B* **2004**, *99*, 511–515. (c) Zhang, G.-Q.; Yang, G.-Q.; Zhu, L.-N.; Chen, Q.-Q.; Ma, J.-S. *Sens. Actuators, B* **2006**, *114*, 995–1000.

(12) For a recent review see: Mashima, K.; Tsurugi, H.; *J. Organomet. Chem.* **2005**, *690*, 4414−4423, and references cited therein.

(13) Holm, R. H.; Chakravorty, A.; Theriot, L. J. *Inorg. Chem.* **1966**, *5*, 625−635, and references cited therein.

(14) For reviews on post-metallocene polymerization catalysts see for example: (a) Ittel, S. D.; Johnson, L. K.; Brookhart, M. *Chem. Rev.* **2000**, *100*, 1169–1203. (b) Britovsek, G. J. P.; Gibson, V. C.; Wass, D. F. *Angew. Chem., Int. Ed.* **1999**, *38*, 428–447. (c) Gibson, V. C.; Spitzmesser, S. K. *Chem. Rev.* **2003**, *103*, 283–315.

(15) Dawson, D. M.; Walker, D. A.; Thornton-Pett, M.; Bochmann, M. *J. Chem. Soc., Dalton Trans.* **2000**, 459–466.

(16) (a) Carabineiro, S. A.; Silva, L. C.; Gomes, P. T.; Pereira, L. C. J.; Veiros, L. F.; Pascu, S. I.; Duarte, M. T.; Namorado, S.; Henriques, R. T. *Inorg. Chem.* **2007**, *46*, 6880–6890. (b) Carabineiro, S. A.; Gomes, P. T.; Veiros, L. F.; Freire, C.; Pereira, L. C. J.; Henriques, R. T.; Warren, J. E.; Pascu, S. I. *Dalton Trans.* **2007**, *46*, 5460–5470. (c) Carabineiro, S. A.; Bellabarba, R. M.; Gomes, P. T.; Pascu, S. I.; Veiros, L. F.; Freire, C.; Pereira, L. C. J.; Henriques, R. T.; Oliveira, M. C.; Warren, J. E. *Inorg. Chem.* **2008**, *47*, 8896–8911.

(17) Bellabarba, R. M.; Gomes, P. T.; Pascu, S. I. *Dalton Trans.* **2003**, 4431–4436.

(18) Pérez-Puente, P.; de Jésus, E.; Flores, J. C.; Gómez-Sal, P. *J. Organomet. Chem.* **2008**, *693*, 3902–3906.

(19) Hao, H.; Bhandari, S.; Ding, Y.; Roesky, H. W.; Magull, J.; Schmidt, H. G.; Noltemeyer, M.; Cui, C. *Eur. J. Inorg. Chem.* **2002**, 1060–1065.

Chart 2. Labeling of Ligand Atoms

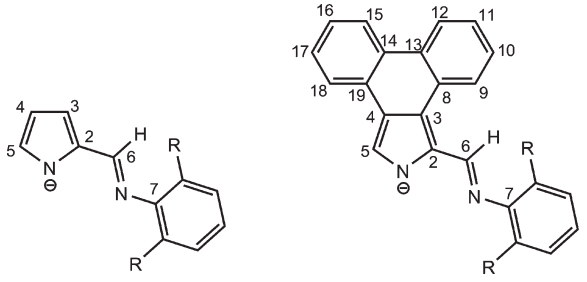

Ia R = H
Ib R = ^{i}Pr

IIa R = H
IIb R = ^{i}Pr

sieves and degassed by the freeze−pump−thaw method. Solvents and solutions were transferred using a positive pressure of nitrogen through stainless steel cannulae, and mixtures were filtered in a similar way using modified cannulae that could be fitted with glass fiber filter disks.

Nuclear magnetic resonance (NMR) spectra were recorded on Varian Unity 300 (^{1}H, 299.995 MHz; ^{13}C, 75.4296 MHz), Bruker Avance III 300 (^{1}H, 300.130 MHz; ^{13}C, 75.4753 MHz) or Bruker Avance III 400 (^{1}H, 400.132 MHz; ^{13}C, 100.623 MHz) spectrometers. Spectra were referenced internally using the residual protio solvent resonance relative to tetramethylsilane ($\delta = 0$). All chemical shifts are quoted in δ (ppm) and coupling constants given in hertz. Multiplicities were abbreviated as follows: broad (br), singlet (s), doublet (d), triplet (t), quartet (q), heptet (h), and multiplet (m). For air- and/or moisture-stable compounds, samples were dissolved in $CDCl_3$ and prepared in common NMR tubes. The NMR assignments of the pyrrole ring or the phenanthro[9,10-*c*]pyrrole rings were made according to the X-ray labeling (see Chart 2). For air- and/or moisture-sensitive materials, samples were prepared in J. Young tubes in a glovebox. Elemental analyses were obtained from the IST elemental analysis services. Mass spectra were collected on a 500 MS LC Ion Trap (Varian, Inc., Palo Alto, CA, U.S.A.) mass spectrometer equipped with an electrospray ionization (ESI) source. The spray voltage was set at ± 5 kV, and the capillary voltage was set at 10 V.

The 2-formiminopyrrole ligand precursors (see below in Scheme 1) were prepared according to previous publications of our group,[16a,17,20] which were adapted from procedures reported in the literature for **Ia**[21,22] and **Ib**,[23,24] by reaction of 2-formylpyrrole with the appropriate aniline, in the presence of a catalytic amount of *p*-toluenesulfonic acid (see Supporting Information). 2-Formylphenanthro[9,10-*c*]pyrrole was synthesized following a method described in the literature[25] with some modifications given in the Supporting Information.

Syntheses of 1-Formiminophenanthro[9,10-*c*]pyrrole Ligand Precursors (IIa,b). A similar procedure used in previous publications of our group was followed.[16a,17,20] Phenanthro[9,10-*c*]-pyrrole-1-carboxaldehyde (10.0 mmol),[25] the appropriate aniline (10 mmol), a catalytic amount of *p*-toluenesulfonic acid and $MgSO_4$ (to remove any water from the reaction mixture) were suspended in absolute ethanol (5 mL) in a 50 mL round-bottom flask, fitted with a condenser and a $CaCl_2$ guard tube. The mixture was heated to reflux overnight turning yellow-orange. After cooling to room temperature, CH_2Cl_2 was added and the suspension was filtered through Celite and washed through with more CH_2Cl_2. After removal of all volatiles, the product was recrystallized in refluxing toluene. The solution, which was stored at −20 °C, yielded 2.24 g (70%) of a light brown solid of **IIa** or 3.16 g (78%) of yellow crystals of **IIb**.

Data for IIa. Anal. Found (calcd) ($C_{23}H_{16}N_2$): C, 86.26 (86.22); H, 5.13 (5.03); N, 8.63 (8.72). NMR [δ_H (400 MHz, $CDCl_3$)]: δ 9.18 (1H, s, N=C*H*), 8.56 (1H, d, J = 2.4 Hz, H15 or H12), 8.50 (1H, d, J = 7.6 Hz, H18 or H9), 8.32 (1H, d, J = 2.0 Hz, H12 or H15), 8.07 (1H, d, J = 6.8 Hz, H9 or H18), 7.79 (1H, s, H5), 7.55−7.43 (6H, m, H10, H11, H16, H17 and aryl *o*-H), 7.33−7.25 (4H, m, aryl *m*- and *p*-H and N*H*); NMR [δ_C (100 MHz, $CDCl_3$)]: δ 151.8 (aryl *ipso*-C), 149.2 (N=*C*H), 130.8 (C14 or C13), 129.4 (aryl *o*-C), 128.4 (C13 or C14), 128.3 (C8 or C19), 128.1 (C19 or C8), 127.3 (C9 or C18), 127.2 (C18 or C9), 126.2 (C16 or C11), 125.62 (aryl *p*-C), 125.6 (C11 or C16), 125.4 (C17 or C10), 125.0 (C4 or C3), 124.1 (C10 or C17), 123.5 (C15 or C12), 122.9 (C12 or C15), 122.5 (C3 or C4), 121.9 (C2), 121.0 (aryl *m*-C), 115.8 (C5). ESI-MS: m/z 321 $[M+H]^+$ (calcd. for $C_{23}H_{17}N_2$ $[M+H]^+$, 321).

Data for IIb. Anal. Found (calcd) ($C_{29}H_{28}N_2$): C, 86.26 (86.10); H, 6.63 (6.98); N, 7.14 (6.92). NMR [δ_H (400 MHz, $CDCl_3$)]: δ 8.95 (1H, s, N=C*H*), 8.56 (1H, d, J = 8.1 Hz, H15 or H12), 8.49 (1H, d, J = 7.8 Hz, H12 or H15), 8.20 (1H, d, J = 7.8 Hz, H18 or H9), 7.98 (1H, d, J = 6.9 Hz, H9 or H18), 7.52−7.43 (4H, m, H10, H11, H16 and H17), 7.40 (1H, s, H5), 7.29−7.23 (4H, m, aryl *m*- and *p*-H and N*H*), 3.20 (2H, hept, J = 6.9 Hz, C*H*$(CH_3)_2$), 1.21 (12H, d, J = 6.9 Hz, CH(C*H*$_3)_2$); NMR [δ_C (100 MHz, $CDCl_3$)]: δ 152.4 (N=*C*H), 149.1 (aryl *ipso*-C), 139.2 (aryl *o*-C), 130.7 (C14 or C13), 129.6 (C13 or C14), 128.4 (C19 or C8), 128.3 (C8 or C19), 128.2 (C3 or C4), 128.1 (C4 or C19), 127.4 (C17 or C10), 127.2 (C10 or C17), 126.2 (C16 or C11), 125.5 (C11 or C16), 125.2 (C18 or C9), 124.7 (aryl *p*-C), 124.1 (C15 or C12), 123.9 (C12 or C15), 123.5 (aryl *m*-C), 122.8 (C9 or C18), 122.2 (C2), 116.5 (C5), 28.1 (*C*H$(CH_3)_2$), 23.7 (CH(*C*H$_3)_2$). ESI-MS: m/z 405 $[M+H]^+$ (calcd. for $C_{29}H_{29}N_2$ $[M+H]^+$, 405).

***In Situ* Synthesis of the Sodium Salts of Compounds Ia,b and IIa,b (IIIa,b and IVa,b).** The same procedure followed in previous publications of the group was used:[16a,17,20] In a typical experiment, NaH (24 mg, 1.0 mmol; or 13 mg, 0.5 mmol) was suspended in THF, and 1 mmol (or 0.5 mmol) of a neutral ligand precursor **Ia**,**b** (or **IIa**,**b**) was slowly added as a solid under a counterflow of nitrogen. An immediate evolution of hydrogen occurred, and after some minutes, a solution of the sodium ligand salt was obtained and stirred for 90 min.

Synthesis of Bis(pyrrole-1-ylmethylene-phenylamine)zinc (1a). Zinc chloride (0.068 g, 0.5 mmol) was suspended in THF and cooled to −78 °C. A solution of sodium salt **IIIa** prepared *in situ* (0.17 g, 1.0 mmol) was filtered and directly added dropwise to the $ZnCl_2$ suspension, which was then stirred for 1 h. The mixture was allowed to warm to room temperature and further stirred overnight. All volatiles were evaporated and the resulting residue was washed with *n*-hexane and extracted with diethyl ether until extracts were colorless. The resulting orange-yellow solution was concentrated and cooled to −20 °C, yielding 0.16 g (80%) of a yellow-orange powder.

Anal. found (calculated) ($C_{22}H_{18}N_4Zn$): C 65.38 (65.44), H 4.79 (4.49), N 13.66 (13.88)%. NMR [δ_H (300 MHz, C_6D_6)]: δ

(20) Gomes, C. S. B.; Suresh, D.; Gomes, P. T.; Veiros, L. F.; Duarte, M. T.; Nunes, T. G.; Oliveira, M. C., *Dalton Trans*., in press, **2009**; DOI: 10.1039/B905948B.
(21) Yeh, K.-N.; Barker, R. H. *Inorg. Chem*. **1967**, *6*, 830–833.
(22) Yoshida, Y.; Matsui, S.; Takagi, Y.; Mitani, M.; Nakano, T.; Tanaka, H.; Kashiwa, N.; Fujita, T. *Organometallics* **2001**, *20*, 4793–4799.
(23) (a) Li, Y.-S.; Li, Y.-R.; Li, X.-F. *J. Organomet. Chem*. **2003**, *667*, 185–191. (b) Antonelli, D. M.; Gomes, P. T.; Green, M. L. H.; Martins, A. M.; Mountford, P. *J. Chem. Soc., Dalton Trans*. **1997**, 2435–2444. (c) Jiménez-Tenorio, M.; Puerta, M. C.; Salcedo, I.; Valerga, P.; Costa, S. I.; Gomes, P. T.; Mereiter, K. *Chem. Commun*. **2003**, 1168–1169. (d) Liu, H.-R.; Costa, S. I.; Gomes, P. T.; Duarte, M. T.; Branquinho, R.; Fernandes, A. C.; Chien, J. C. W.; Marques, M. M. *J. Organomet. Chem*. **2005**, *690*, 1314–1323.
(24) Iverson, C. N.; Carter, C. A. S. G.; Baker, R. T.; Scollard, J. D.; Labinger, J. A.; Bercaw, J. E. *J. Am. Chem. Soc*. **2003**, *125*, 12674–12675.
(25) (a) Lash, T. D.; Chandrasekar, P.; Osuma, A. T.; Chaney, S. T.; Spence, J. D. *J. Org. Chem*. **1998**, *63*, 8455–8469. (b) Novak, B. H.; Lash, T. D. *J. Org. Chem*. **1998**, *63*, 3998–4010. (c) Lash, T. D.; Bellettini, J. R.; Bastian, J. A.; Couch, K. B. *Synthesis* **1994**, 170–172.

8.20 (2H, s, N=C*H*), 7.42−7.40 (2H, m, H5), 7.28−7.26 (2H, m, H3), 7.18−7.10 (4H, m, aryl *o*-H), 7.03−7.01 (2H, m, H4), 6.87−6.285 (6H, m, aryl *m*- and *p*-H); NMR [δ_H (300 MHz, C_6D_6)]: δ 154.1 (N=*C*H), 147.0 (aryl *ipso*-C), 138.6 (C5), 138.1 (C2), 129.6 (aryl *m*-C), 125.6 (aryl *p*-C), 121.6 (C3), 120.5 (aryl *o*-C), 115.6 (C4). ESI-MS: *m*/*z* 403 $[M+H]^+$ (calcd. for $C_{22}H_{19}N_4Zn$ $[M+H]^+$, 403).

Synthesis of Bis(pyrrole-1-ylmethylene-(2,6-diisopropylphenyl)amine)zinc (1b). This compound was already reported in the literature, although synthesized by a different method.[19] The same procedure described for **1a** was followed, using a solution of sodium salt **IIIb** prepared *in situ* (0.25 g, 1.0 mmol), to give 0.13 g (44%) of a pale yellow powder.

Anal. found (calculated) ($C_{34}H_{42}N_4Zn$): C 71.29 (71.38), H 7.49 (7.40), N 9.96 (9.79)%. NMR [δ_H (300 MHz, C_6D_6)]: δ 7.49 (2H, s, N=C*H*), 7.12 (2H, br s, H5), 6.98−6.92 (6H, m, aryl *m*- and *p*-H), 6.84 (2H, dd, J_1 = 3.6 Hz, J_2 = 1.2 Hz, H3), 6.55 (2H, dd, J_1 = 3.6 Hz, J_2 = 1.5 Hz, H4), 3.13 (4H, h, J = 6.6 Hz, C*H*(CH_3)$_2$), 1.06 (12H, d, J = 6.6 Hz, CH(C*H*$_3$)$_2$), 0.60 (12H, d, J = 6.6 Hz, CH(C*H*$_3$)$_2$). NMR [δ_C (75 MHz, C_6D_6)]: δ 161.3 (N=*C*H), 144.9 (aryl *ipso*-C), 141.9 (aryl *o*-C), 137.6 (C2), 136.6 (aryl *p*-C), 126.2 (C5), 124.0 (aryl *m*-C), 120.7 (C3), 115.1 (C4), 28.4 (*C*H(CH_3)$_2$), 24.6 (CH(*C*H$_3$)$_2$), 23.0 (CH(*C*H$_3$)$_2$). ESI-MS: *m*/*z* 571 $[M+H]^+$ (calcd. for $C_{34}H_{43}N_4Zn$ $[M+H]^+$, 571).

Synthesis of Bis(phenanthro[9,10-*c*]pyrrole-1-ylmethylene-phenylamine)zinc (2a). Procedure A. The same procedure described for **1a** was followed, but a solution of sodium salt **IVa** prepared *in situ* (0.16 g, 0.5 mmol) was employed. Extraction of the reaction products with toluene, until extracts remained colorless, and removal of the solvent by vacuum evaporation, afforded a yellow-mustard powder, which was recrystallized in CH_2Cl_2 and double-layered with *n*-hexane, at −20 °C, giving 0.88 g (50%) of a bright green powder.

Procedure B. A solution of 1-formiminophenanthro[9,10-*c*]-pyrrole **IIa** (0.32 g, 1.0 mmol) in a mixture of solvents, toluene (25 mL), and THF (10 mL), was added to a solution of $ZnMe_2$ (0.5 mL of a 2.0 M solution in toluene, 1.0 mmol) diluted with toluene (20 mL), at −80 °C. After the addition, the mixture was warmed slowly to room temperature and stirred overnight. All volatiles were evaporated, and the resulting residue was washed with *n*-hexane and extracted with toluene until the extracts were colorless. The remaining residue was extracted with THF and filtered. The resulting yellow-greenish solutions were evaporated, and the residue redissolved in toluene, double-layered with *n*-hexane, and cooled to −20 °C, to yield 0.34 g (95% based on **IIa**) of a yellow-green powder.

Anal. Found (calcd) ($C_{46}H_{30}N_4Zn$): C 78.92 (78.46), H 4.02 (4.29), N 8.12 (7.96). NMR [δ_H (300 MHz, CD_2Cl_2)]: δ 9.47 (2H, s, N=C*H*), 8.68 (2H, d, J = 8.1 Hz, H15 or H12), 8.58 (2H, d, J = 8.1 Hz, H18 or H9), 8.53 (2H, d, J = 8.4 Hz, H12 or H15), 8.23 (2H, s, H5), 8.15 (2H, d, J = 6.6 Hz, H9 or H18), 7.67−7.49 (8H, m, H10, H11, H16 and H17), 7.33−7.24 (6H, m, aryl *m*- and *p*-H), 7.10−7.08 (4H, m, aryl *o*-H); NMR [δ_H (300 MHz, C_6D_6)]: δ 9.14 (2H, s, N=C*H*), 8.54 (2H, dd, J = 6.9 Hz, J = 2.4 Hz, H15 or H12), 8.47 (2H, dd, J = 8.4 Hz, J = 1.2 Hz, H18 or H9), 8.36 (2H, dd, J = 6.3 Hz, J = 2.4 Hz, H12 or H15), 8.08 (2H, dd, J = 7.5 Hz, J = 1.5 Hz, H9 or H18), 7.84 (2H, s, H5), 7.48−7.35 (8H, m, H10, H11, H16 and H17), 6.97−6.88 (6H, m, aryl *m*- and *p*-H), 6.80−6.75 (4H, m, aryl *o*-H). NMR [δ_C (75 MHz, CD_2Cl_2)]: δ 160.7 (aryl *ipso*-C), 152.4 (N=*C*H), 139.2 (aryl *o*-C), 133.6 (C14 or C13), 130.8 (C13 or C14), 128.6 (C8 or C19), 128.4 (C19 or C8), 127.8 (C9 or C18), 127.6 (C18 or C9), 126.6 (C16 or C11), 126.2 (C4 or C3), 126.0 (C11 or C16), 125.7 (C17 or C10), 125.0 (C4 or C3), 124.7 (aryl *p*-C), 124.4 (C10 or C17), 123.9 (C15 or C12), 123.6 (aryl *m*-C), 123.3 (C12 or C15), 122.7 (C2), 116.2 (C5). ESI-MS: *m*/*z* 703 $[M+H]^+$ (calcd. for $C_{46}H_{31}N_4Zn$ $[M+H]^+$, 703).

Synthesis of Bis(phenanthro[9,10-*c*]pyrrole-1-ylmethylene-(2,6-diisopropylphenyl)amine)zinc (2b). The same procedures described for **2a** were followed.

Table 1. Crystal Data and Structure Refinement for Compounds **IIb** and **2b**

	IIb	**2b**
formula	$C_{29}H_{28}N_2$	$C_{58}H_{54}N_4Zn$
M	404.53	872.42
λ/ Å	0.71073	0.71073
T/ K	150	150
crystal system	monoclinic	monoclinic
space group	$P2_1/c$	Cc
a/ Å	12.6922 (12)	16.105(8)
b/ Å	20.6575 (21)	12.486(7)
c/ Å	8.8788 (9)	24.603(13)
α/ deg	90	90
β/ deg	108.119 (6)	108.52(3)
γ/ deg	90	90
V/ Å^3	2212.5 (4)	4691(4)
Z	4	4
ρ_{calc}/ g cm^{-3}	1.214	1.235
μ/ mm^{-1}	0.071	0.566
θ_{max}/ deg	25.74	25.03
total data	30099	37322
unique data	4179	7901
R_{int}	0.1099	0.3488
R [$I > 3\sigma(I)$]	0.0628	0.0898
wR	0.1484	0.1710
goodness of fit	1.013	0.835
ρ min, ρ max	−0.407	−0.360
	0.519	0.441

Procedure A. A solution of sodium salt **IVb** prepared *in situ* (0.20 g, 0.5 mmol) was employed. After extraction of the reaction products with toluene, the resulting solution was concentrated and stored at −20 °C, giving 0.15 g (70%) of a bright yellow powder.

Procedure B. A solution of 1-formiminophenanthro[9,10-*c*]-pyrrole **IIb** (0.20 g, 0.5 mmol) in a mixture of solvents, toluene (10 mL), and THF (5 mL) was added to a solution of $ZnMe_2$ (0.25 mL of a 2.0 M solution in toluene, 0.5 mmol) diluted with toluene (10 mL), at −80 °C. After the addition, the mixture was warmed slowly to room temperature and stirred overnight. All volatiles were evaporated, and the resulting residue was washed with *n*-hexane and extracted with toluene. The resulting bright yellow solution was evaporated, redissolved in toluene, double-layered with *n*-hexane and cooled to −20 °C, to yield 0.19 g (89% based on **IIb**) of a yellow powder.

Anal. Found (calcd) ($C_{58}H_{54}N_4Zn$): C 79.63 (79.85), H 6.55 (6.24), N 6.13 (6.42). NMR [δ_H (300 MHz, CD_2Cl_2)]: δ 8.80 (2H, s, N=C*H*), 8.66 (2H, d, J = 7.8 Hz, H15 or H12), 8.58 (2H, d, J = 7.8 Hz, H12 or H15), 8.27 (2H, d, J = 8.4 Hz, H18 or H9), 8.21−8.19 (4H, m, H9 or H18 and H16 or H11), 7.58−7.48 (8H, m, H10, H11 or H16, H17 and aryl *p*-H), 7.16−7.06 (6H, m, H5 and aryl *m*-H), 3.23 (4H, br s, C*H*(CH_3)$_2$), 1.20 (12H, d, J = 6.6 Hz, CH(C*H*$_3$)$_2$), 0.52 (12H, d, J = 6.3 Hz, CH(C*H*$_3$)$_2$); NMR [δ_H (300 MHz, C_6D_6)]: δ 8.85 (2H, s, N=C*H*), 8.46 (2H, d, J = 8.0 Hz, H15 or H12), 8.43 (2H, d, J = 8.5 Hz, H12 or H15), 8.24 (2H, d, J = 7.8 Hz, H18 or H9), 8.14 (2H, d, J = 7.6 Hz, H9 or H18), 8.04 (2H, s, H5), 7.44 (2H, t, J = 7.1 Hz, H16 or H11), 7.38−7.27 (6H, m, H10, H11 or H16 and H17), 7.05−6.95 (6H, m, aryl *m*- and *p*-H), 3.28 (4H, br s, C*H*(CH_3)$_2$), 1.15 (24H, d, J = 6.8 Hz, CH(C*H*$_3$)$_2$). NMR [δ_C (75 MHz, CD_2Cl_2)]: δ 161.0 (N=*C*H), 145.0 (aryl *ipso*-C), 142.4 (aryl *o*-C), 132.1 (C9 and C18), 131.2 (C13 or C14), 130.8 (C14 or C13), 129.2 (C8 or C19), 128.6 (C19 or C8), 128.1 (C4 or C3), 127.6 (C17 or C10), 127.4 (C10 or C17), 127.1 (C3 or C4), 127.0 (C2), 126.5 (C16 or C11), 126.3 (C11 or C16), 125.1 (aryl *p*-C), 124.5 (C15 and C12), 124.4 (aryl *m*-C), 123.8 (C12 or C15), 123.3 (C5), 28.7 (*C*H(CH_3)$_2$), 24.8 (CH(*C*H$_3$)$_2$), 23.0 (CH(*C*H$_3$)$_2$). ESI-MS: *m*/*z* 871 $[M+H]^+$ (calcd. for $C_{58}H_{55}N_4Zn$ $[M+H]^+$, 871).

X-ray Experimental Data. Crystallographic and experimental details of crystal structure determinations are listed in Table 1. The crystal of complex **2b** was selected under an inert atmosphere,

covered with polyfluoroether oil, and mounted on a nylon loop. Crystallographic data for the ligand precursor **IIb** and complex **2b** were collected using graphite monochromated Mo Kα radiation ($\lambda = 0.71073$ Å) on a Bruker AXS-KAPPA APEX II diffractometer equipped with an Oxford Cryosystems open-flow nitrogen cryostat, at 150 K. Cell parameters were retrieved using Bruker SMART software and refined using Bruker SAINT on all observed reflections. Absorption corrections were applied using SADABS.[26] Structure solution and refinement were performed using direct methods with the programs SIR97[27] and SHELXL[28] both included in the package of programs WINGX-Version 1.70.01.[29] For compound **2b**, the poor diffracting power, size, and crystal quality ($R_{int} = 0.3488$) prevented the anisotropic refinement of all the non-hydrogen atoms. Only Zn and the N atoms were refined with anisotropic displacement parameters. Because of the number of atoms present in the asymmetric unit, the anisotropic refinement would lead to a very poor ratio of number of refined parameters/number of reflections that could prevent a good, stable, and reliable refinement. When analyzing the diffraction data, a very low value of $|E^2 - 1| = 0.541$ indicated the presence of twinning. Using the program TwinRotMat routine included in PLATON,[30] we determined a possible twin matrix, indicating general and racemic twinning. The TWIN law used was −1 0 0 0 −1 0 1 0 1 and the BASF components refined equally to 0.17. All hydrogen atoms, except the NH proton in **IIb**, were inserted in idealized positions and allowed to refine riding on the parent carbon atom. Figures were generated using ORTEP3.[31] Data was deposited in CCDC under the deposit numbers 742158 for **IIb** and 742157 for **2b**.

Photophysical Characterization. Solution samples were prepared in a glovebox by dissolving the complexes (or the ligand precursors) in freshly distilled THF (dried over sodium under nitrogen). Their concentrations (c) were: [**Ia**] = 5.2×10^{-6} M, [**Ib**] = 5.4×10^{-6} M, [**1a**] = 9.9×10^{-6} M, and [**1b**] = 7.1×10^{-6} M; [**IIa**] = 9.5×10^{-6} M, [**IIb**] = 5.6×10^{-6} M, [**2a**] = 3.4×10^{-6} M, and [**2b**] = 9.4×10^{-7} M. The solutions were kept in quartz cells, under inert atmosphere. Absorption and fluorescence spectra were recorded with a Beckman DU-70 spectrophotometer and a SPEX Fluorolog 212I fluorimeter, respectively. The fluorescence spectra were corrected for the wavelength response of the instrumental system. Fluorescence quantum yields (ϕ_f) were measured using α-oligothiophenes as standards.[32] Fluorescence decays were measured using the time-correlated single-photon counting (TCSPC) technique with picoseconds resolution (excitation pulse fwhm = 19 ps). The experimental setup employed is described elsewhere.[33]

Computational Details. DFT calculations[34] were performed using the Amsterdam Density Functional (ADF) program package.[35] Gradient corrected geometry optimizations,[36] without symmetry constraints, were performed using the local density approximation of the correlation energy (Vosko−Wilk−Nusair),[37] and the generalized gradient approximation (Becke's exchange[38] and Perdew's correlation functionals[39]). The core orbitals were frozen for Zn ([1−2]s, 2p); C and N (1s). Triple ζ Slater-type orbitals (STO) were used to describe the valence shells of C, N (2s and 2p), and Zn (3d, 4s). A set of two polarization functions was added to C, N (single ζ, 3d, 4f), and Zn (single ζ, 4p, 4f). Triple ζ Slater-type orbitals (STO) were used to describe the valence shells of H (1s) with two polarization function (single ζ, 2s, 2p). Relativistic effects were treated with the ZORA approximation.[40] TD-DFT calculations[41] with the ADF implementation were used to determine the excitation energies. The 10 lowest singlet−singlet excitation energies for **L1** and **L2** and the 40 lowest singlet−singlet excitation energies for **C1** and **C2** were calculated, using the optimized geometries. Unrestricted calculations were performed for the first excited singlet state structure, obtained from a HOMO (H) to LUMO (L) excitation, which was fully optimized without symmetry constraints. The solvent effects were included using the COnductor like Screening Model (COSMO)[42,43] implemented in ADF on the gas phase optimized structures. Three-dimensional representations of the orbitals were obtained with Molekel,[44] and structures and electronic spectra with Chemcraft.[45]

Results and Discussion

Synthesis of Complexes. The formiminopyrrole ligand precursors **Ia**,**b** and **IIa**,**b** herein reported (Scheme 1) were prepared and characterized according to a method described in previous publications.[16a,17,20] It consists in the condensation of 2-formylpyrrole or 2-formylphenanthro[9,10-*c*]-pyrrole with two types of arylamines (aniline or 2,6-diisopropylaniline), employing standard conditions.[15−17,21−24]

Despite that 2-formylpyrrole is available commercially, its preparation from pyrrole, dimethylformamide (DMF), and phosphorus oxychloride is a straightforward reaction, known as the Vilsmeier−Haak acylation.[46] This formylation reaction is also employed in the last step of the preparation of 2-formylphenanthro[9,10-*c*]pyrrole from phenanthro[9,10-*c*]pyrrole. However, the prepara-

(26) Sheldrick, G. M. *SADABS, Program for Empirical Absorption Correction*; University of Göttingen: Göttingen, Germany, 1996.
(27) *SIR97*; Altomare, A.; Burla, M. C.; Camalli, M.; Cascarano, G. L.; Giacovazzo, C.; Guagliardi, A.; Moliterni, A. G. G.; Polidori, G.; Spagna, R. *J. Appl. Crystallogr.* **1999**, *32*, 115−119.
(28) Sheldrick, G. M. *SHELX97 - Programs for Crystal Structure Analysis* (*Release 97−2*); Institüt für Anorganische Chemie der Universität: Tammanstrasse 4, D-3400 Göttingen, Germany, 1998.
(29) Farrugia, L. J. *J. Appl. Crystallogr.* **1999**, *32*, 837–838.
(30) (a) Spek, A. L. *Acta Crystallogr., Sect. A* **1990**, *C34*, 46. (b) *PLATON, A Multipurpose Crystallographic Tool*; Utrecht University: Utrecht, The Netherlands, Spek, A. L., 1998.
(31) *ORTEP3 for Windows*; Farrugia, L. J. *J. Appl. Crystallogr.* **1997**, *30*, 565.
(32) Becker, R. S.; de Melo, J. S.; Maçanita, A. L.; Elisei, F. *Pure Appl. Chem.* **1995**, *67*, 9–16.
(33) Di Paolo, R. E.; Burrows, H. D.; Morgado, J.; Maçanita, A. L. *ChemPhysChem* **2009**, *10*, 448–454.
(34) Parr, R. G.; Young, W. *Density Functional Theory of Atoms and Molecules*; Oxford University Press: New York, 1989.
(35) (a) Velde, G. T.; Bickelhaupt, F. M.; Baerends, E. J.; Guerra, C. F.; van Gisbergen, S. J. A.; Snijders, J. G.; Ziegler, T. *J. Comput. Chem.* **2001**, *22*, 931–967. (b) Guerra, C. F.; Snijders, J. G.; Velde, G. T.; Baerends, E. J. *Theor. Chem. Acc.* **1998**, *99*, 391–403. (c) *ADF2005.01*; SCM, Theoretical Chemistry, Vrije Universiteit: Amsterdam, The Netherlands.
(36) (a) Versluis, L.; Ziegler, T. *J. Chem. Phys.* **1988**, *88*, 322–328. (b) Fan, L. Y.; Ziegler, T. *J. Chem. Phys.* **1991**, *95*, 7401–7408.
(37) Vosko, S. H.; Wilk, L.; Nusair, M. *Can. J. Phys.* **1980**, *58*, 1200.
(38) Becke, A. D. *J. Chem. Phys.* **1987**, *88*, 1053–1062.
(39) (a) Perdew, J. P. *Phys. Rev. B* **1986**, *33*, 8822–8824. (b) Perdew, J. P. *Phys. Rev. B* **1986**, *34*, 7406.
(40) van Lenthe, E.; Ehlers, A.; Baerends, E. J. *J. Chem. Phys.* **1999**, *110*, 8943–8953.
(41) (a) van Gisbergen, S. J. A.; Groeneveld, J. A.; Rosa, A.; Snijders, J. G.; Baerends, E. J. *J. Phys. Chem. A* **1999**, *103*, 6835–6844. (b) Rosa, A.; Baerends, E. J.; van Gisbergen, S. J. A.; van Lenthe, E.; Groeneveld, J. A.; Snijders, J. G. *J. Am. Chem. Soc.* **1999**, *121*, 10356–10365. (c) van Gisbergen, S. J. A.; Rosa, A.; Ricciardi, G.; Baerends, E. J. *J. Chem. Phys.* **1999**, *111*, 2499–2506.
(42) (a) Klamt, A.; Schüürmann, G. *J. Chem. Soc., Perkin Trans. 2* **1993**, 799–805. (b) Klamt, A. *J. Phys. Chem.* **1995**, *99*, 2224–2235. (c) Klamt, A.; Jonas, V. *J. Chem. Phys.* **1996**, *105*, 9972–9981.
(43) (a) Dunning, T. H., Jr.; Hay, P. J. *Modern Theoretical Chemistry*; Plenum Press: New York, 1977; Vol. *3*, pp 1−27. (b) Hay, P. J.; Wadt, W. R. *J. Chem. Phys.* **1985**, *82*, 270–283. (c) Hay, P. J.; Wadt, W. R. *J. Chem. Phys.* **1985**, *82*, 299–310.
(44) Portmann, S.; Lüthi, H. P. *Chimia* **2000**, *54*, 766–770.
(45) http://www.chemcraftprog.com/index.html.
(46) Gayido, D. O. A.; Buldain, G.; Frydman, B. *J. Org. Chem.* **1984**, *49*, 2619–2622.

Scheme 1. Syntheses of the Ligand Precursors

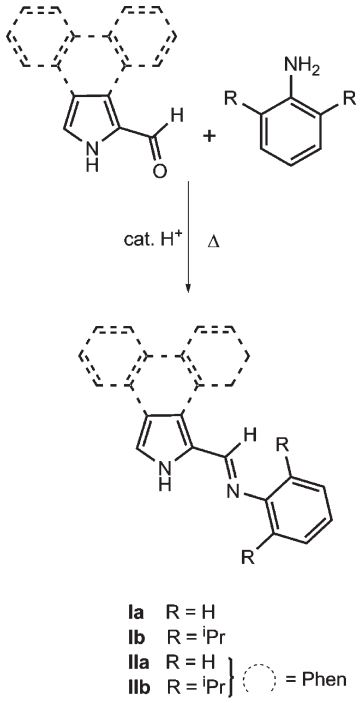

tion of the latter compound consisted of a sequence of several steps starting from phenanthrene, in a synthetic sequence slightly adapted from the literature[25] (see Supporting Information). The corresponding formimines were obtained as powder or crystalline materials, with colors ranging from pale yellow to light brown and yields varying from 70 to 78%. These ligand precursors were characterized by ^{1}H and $^{13}C\{^{1}H\}$ NMR spectroscopy. The crystal structure of ligand precursor **IIb** was determined (see X-ray Diffraction Section).

Treatment of the ligand precursors **Ia**,**b** and **IIa**,**b** with sodium hydride, in THF, resulted in the deprotonation of the NH proton of the pyrrole ring and consequent formation of either the pyrrolyl or the phenanthro[9,10-*c*]-pyrrolyl sodium salts, respectively, **IIIa**,**b** and **IVa**,**b**. These sodium salts were prepared *in situ* and subsequently reacted with the corresponding metal halides.

Slow addition of a THF solution of salts **IIIa**,**b** or **IVa**,**b** prepared *in situ* to a suspension of $ZnCl_2$ in the same solvent, in a molar ratio of 2:1 (ligand precursor:$ZnCl_2$), gave rise to complexes **1a**,**b** and **2a**,**b** (Scheme 2, route A). The zinc complexes formed in the reaction were extracted with diethyl ether, in the case of the simple iminopyrrolyl ligand derivatives, or with toluene, for the iminophenanthro-[9,10-*c*]pyrrolyl ones. Further workup yielded powders with colors orange-yellow (**1a**), pale yellow (**1b**), bright green (**2a**) and bright yellow (**2b**), in moderate to high yields (80, 44, 50 and 70%, respectively). Deprotonation of the ligand precursors with *n*-LiBu followed by reaction with $ZnCl_2$ was also attempted, but lower yields than those produced with NaH were obtained. All compounds showed to be sensitive to air and moisture, either in solid or in solution. This instability was also observed in the case of the related zinc complexes prepared by Wang et al.[47]

(47) Liu, S.-F.; Wu, Q.; Schmider, H. L.; Aziz, H.; Hu, N.-X.; Popović, Z.; Wang, S. *J. Am. Chem. Soc.* **2000**, *122*, 3671–3678.

Scheme 2. Synthetic Routes Used in the Present Work for the Syntheses of Zinc Complexes[a]

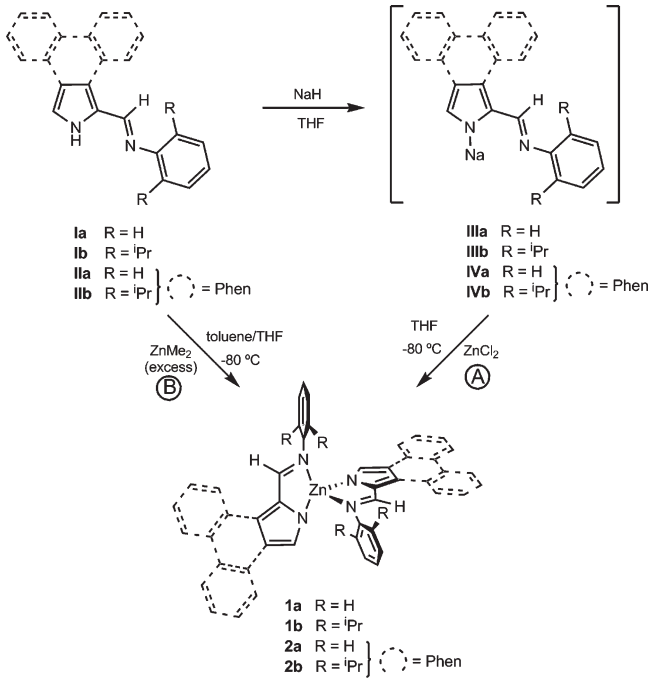

[a] Route B was only employed for phenanthro[9,10-*c*]iminopyrrolyl derivatives. Sodium derivatives were generated *in situ*.

Compound **1b** has already been described in the literature by Roesky et al.,[19] being prepared by reaction of an excess of $ZnMe_2$ with the protonated ligand precursor **Ib**, in a toluene/*n*-hexane solvent mixture. However, a low yield was reported (20%) in comparison with that of the present reaction of $ZnCl_2$ with **IIIb** (44%). In this work, complexes **2a**,**b** were also synthesized via the $ZnMe_2$ method (Scheme 2, route B). The use of a toluene/THF solvent mixture (instead of toluene/*n*-hexane) led to the improved syntheses of formiminophenanthro[9,10-*c*]pyrrolyl zinc complexes **2a** and **2b**, which were obtained in very high yields (95 and 89%, respectively).

X-ray Diffraction. For compounds **IIb** and **2b**, crystals suitable for X-ray diffraction were obtained, allowing the determination of their crystal structures. Compound **IIb** crystallizes in the space group $P2_1/c$. The molecular structure of the ligand precursor **IIb** is represented in Figure 1, and selected bond distances and angles are listed in Table 2. The asymmetric unit of compound **IIb** contains a single molecule.

For compound **IIb**, the phenanthro[9,10-*c*]pyrrole system shows a planar backbone, where the phenanthrene moiety displays the usual delocalized π system and the longest and shortest bonds in the pyrrole ring are C(3)−C(4) (1.417(4) Å) and N(1)−C(5) (1.350(3) Å), respectively, as can be seen in Table 2. The angle centered at N(1) is 111.3(2)°, while that at N(2) is 118.3(2)°. The imine N(2)−C(6) exhibits a distance of 1.276(3) Å, which is typical for this type of groups.[16,17,20] The coplanarity of the phenanthro[9,10-*c*]pyrrole backbone with the formimino group (torsion angle N(2)−C(6)−C(2)−N(1) of 3.4(4)°) and a distance C(2)−C(6) (1.429(4) Å) shorter than normal values for typical C−C single bond, points to an extension of the pyrrole ring π-electronic

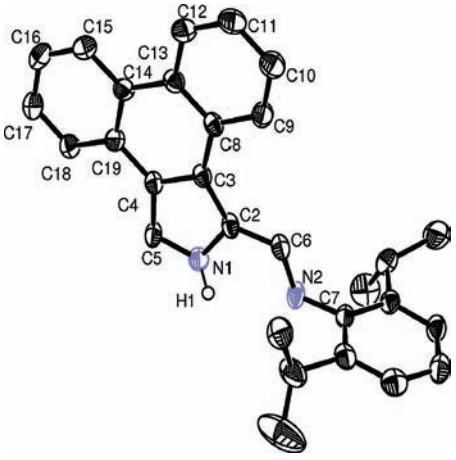

Figure 1. ORTEP III diagram of the ligand precursor **IIb** using 50% probability level ellipsoids. Calculated hydrogen atoms have been omitted for clarity.

Table 2. Selected Bond Distances (Å) and Angles (deg) for the Ligand Precursor **IIb**

parameter	**IIb**
Distances (Å)	
N(1)−C(2)	1.373(3)
N(1)−C(5)	1.350(3)
C(3)−C(2)	1.412(4)
C(3)−C(4)	1.417(4)
C(5)−C(4)	1.381(4)
C(6)−C(2)	1.429(4)
N(2)−C(6)	1.276(3)
N(2)−C(7)	1.427(3)
Angles (deg)	
C(6)−N(2)−C(7)	118.3(2)
N(1)−C(2)−C(6)	118.5(2)
N(2)−C(6)−C(2)	121.8(3)
C(3)−C(2)−C(6)	134.9(2)
N(1)−C(2)−C(3)	106.5(2)
C(2)−C(3)−C(4)	106.5(2)
C(5)−C(4)−C(3)	108.1(2)
N(1)−C(5)−C(4)	107.6(2)
C(5)−N(1)−C(2)	111.3(2)

delocalization toward its formimino substituent. In this compound, the steric hindrance produced by the two bulky isopropyl substituents, at the 2 and 6 positions of the phenyl ring, makes it nearly perpendicular (80.50°) to the formiminophenanthro[9,10-*c*]pyrrole plane defined by atoms N(2)−C(6)−C(2)−N(1). The supramolecular arrangement shows dimerization of the iminopyrrole molecules, which are coplanar and connected by complementary hydrogen bonds between the imino group and the pyrrole NH of the adjacent molecule.[48] One can also observe π-stacking of the phenanthrene rings of adjacent dimers (Figure 2).

Complex **2b** crystallized in the monoclinic *Cc* space group. Its X-ray molecular structure reveals a distorted tetrahedral geometry about the Zn atom with the four nitrogen atoms of two chelating 2-formiminophenanthro[9,10-*c*]pyrrolyl ligands arranged at the vertices

(48) Munro, O. Q.; Joubert, S. D.; Grimmer, C. D. *Chem.—Eur. J.* **2006**, *12*, 7987–7999.

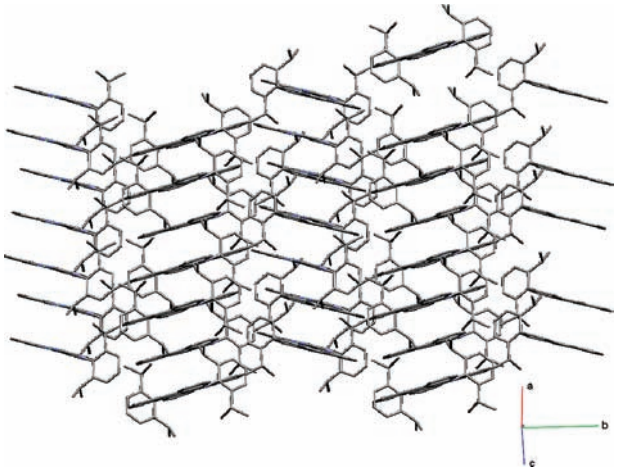

Figure 2. Crystal packing structure of ligand precursor **IIb**.

(see Supporting Information, Figure S1 and Table S1). However, only the Zn and the N atoms were refined with anisotropic displacement parameters because of the poor quality of the crystal (see Experimental Section).

Photophysical Characterization. The 2-aryliminopyrrole ligand precursors **Ia** and **Ib** (emission bands at λ_{max} = 357 and 322 nm, respectively) show negligible fluorescence quantum yields ($\leq$0.07%) in THF. The coordination of the resulting 2-aryliminopyrrolyl ligands in complexes **1a** and **1b** exhibit slightly higher fluorescence quantum yields (ϕ_f) in relation to **Ia** and **Ib**, the corresponding values (ϕ_f = 0.26 and 0.16%) being close to those obtained by Ma et al.[11b] for a related iminopyrrolyl Zn system studied for applications as Zn^{2+} sensor. Absorption and fluorescence spectra, as well as photophysical data for **Ia**,**b** and **1a**,**b** are shown in the Supporting Information, Figure S2 and Table S2.

Absorption and emission spectra of the 2-aryliminophenanthro[9,10-*c*]pyrrole ligand precursors (**IIa** and **IIb**) and their corresponding Zn complexes (**2a** and **2b**) are shown in Figure 3, and their photophysical properties such as the absorption and emission maxima wavelengths (λ_{abs} and λ_{em}, respectively), molar extinction coefficient (ε_{max}), fluorescence quantum yields and average fluorescence lifetimes ($\langle\tau_f\rangle$) are listed in Table 3. Radiative k_f and radiationless k_{nr} rate constants derived from fluorescence quantum yields and lifetimes are also shown.

The absorption spectra of compounds of the type **a** (aryl = phenyl) are substantially red-shifted (ca. 15 and 40 nm, for ligand precursors and complexes, respectively) with respect to those of the type **b** (aryl = 2,6-diisopropylphenyl), indicating extension of the delocalized π-orbitals to the phenyl group in compounds **a**. This delocalization occurs to a lesser extent in compounds **b** because of the expectable larger dihedral angle of the 2,6-diisopropylphenyl ring in relation to the iminopyrrole/yl backbone, resulting from the high steric hindrance of the isopropyl groups. This effect has already been observed in the molecular structures of the simple iminopyrrolyl ligand precursors **Ia** and **Ib**.[20]

Another interesting observation is the red-shift of the absorption spectra of complexes **2a** and **2b** (65 and 36 nm, respectively) relative to those of the corresponding ligand precursors (Table 3). These large shifts suggest an

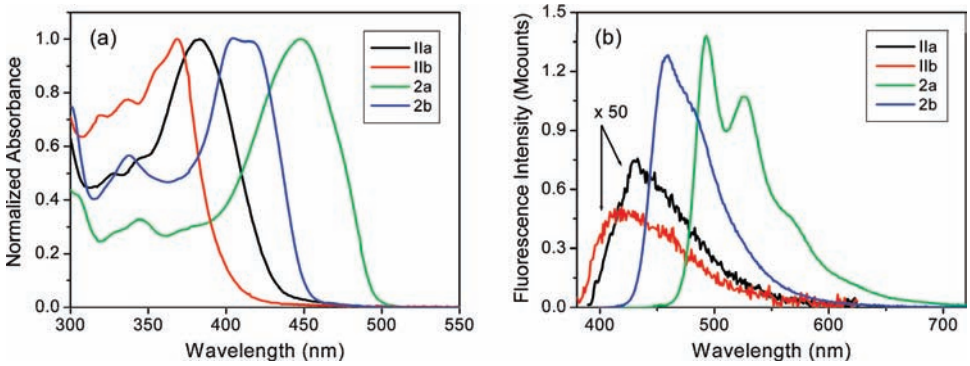

Figure 3. Normalized (a) absorption and (b) fluorescence spectra of ligand precursors **IIa**,**b** and complexes **2a**,**b** (for each compound, obtained by exciting at its absorption maximum wavelength), in THF, at 293 °C. The ligand precursors fluorescence spectra are magnified 50-fold for better visibility.

Table 3. Photophysical Parameters of Zn Complexes **2a** and **2b** and of Their Corresponding Neutral Ligand Precursors **IIa** and **IIb**, in THF, at 293 K

compound	λ_{abs} (nm)	$\varepsilon_{max} \times 10^{-4}$ (L mol^{-1} cm^{-1})	λ_{em} (nm)	ϕ_f (%)	$\langle\tau_f\rangle^a$ (ps)	$\tau_{rad}{}^b$ (ns)	$k_f \times 10^{-7\,c}$ (s^{-1})	$k_{nr} \times 10^{-9\,d}$ (s^{-1})
IIa	383	2.9	432	0.16	425	263	0.38	2.4
IIb	369	1.6	419	0.23	532	233	0.43	1.9
2a	448	2.0	494	8.8	435	4.8	21	2.2
2b	405	4.2	459	3.9	180	4.8	21	5.2

$^a\langle\tau_f\rangle = \sum a_i\,\tau_i$. $^b\tau_{rad} = 1/k_f$. $^c k_f = \phi_f/\langle\tau_f\rangle$. $^d k_{nr} = (1 - \phi_f)/\langle\tau_f\rangle$.

enhancement of the π-conjugation due to the bidentate complexation of the ligand to the d^{10} spectroscopically inactive Zn^{2+} ion. The bidentate coordination imposes a planar conformation in the iminopyrrolyl backbone by restricting the rotation about the C2−C6 bond.

The fluorescence spectra of complexes **2a** and **2b** show red-shifts (62 and 40 nm, respectively) relative to the ligand precursors, similar to those observed in the absorption spectra. As in the case of absorption, these red shifts may be attributed to the highly resonant π-conjugated framework of the deprotonated iminophenanthropyrrole ligand precursor, giving rise to a decrease in the $\pi^*-\pi$ energy gap of the ligand molecular orbitals responsible for the transitions.[49,50] More importantly, a substantial increase (ca. 60 and 20-fold, respectively) in the fluorescence quantum yields, ϕ_f, is observed. This is in accordance with the results obtained by other authors for the spectroscopic properties observed with other zinc complexes and corresponding ligand precursors.[47,49,51]

Fluorescence decays of complexes **2a** and **2b** were measured at two emission wavelengths of the onset and tail of the fluorescence bands (see Supporting Information, Figure S4). The decay times were well fitted with double exponential functions, being the average fluorescence lifetimes listed in Table 3. The decays of the ligand precursors **IIa** and **IIb** (see Supporting Information, Figure S3), measured at a single emission wavelength, were also obtained as multiexponentials with average fluorescence lifetimes indicated in Table 3.

The values of the radiative k_f and radiationless rate constants k_{nr} (Table 3) show that the fluorescence quantum yields enhancement in the complexes results from a 50-fold increase in the radiative rate constant values (k_{nr} values are similar for all four compounds). This indicates a much more allowed transition (larger transition dipole moment) from the first singlet excited state (S_1) to the ground state (S_0) in the case of the complexes. In fact, the k_f values of the complexes are typical of allowed transitions, and are consistent with the order of magnitude of their ε_{max} values (also proportional to the transition dipole moment), while those of the ligand precursors are typical of forbidden transitions. The ε_{max} values of both complexes and ligands are of the same order of magnitude, which strongly indicates that the $S_1 \rightarrow S_0$ transition, in the case of the ligand precursors, does not correspond to the main absorption band (where ε_{max} was measured). In fact, the absorption spectra of the ligand precursors show long wavelength tails (e.g., ε_{459nm} = 580 L mol^{-1} cm^{-1} and ε_{403nm} = 832 L mol^{-1} cm^{-1}, for **IIa** and **IIb**, respectively) that are absent in the complexes. These tails are due to the presence of transitions with strong $n-\pi^*$ character resulting from the excitation of a nitrogen lone pair electron to a delocalized π^* orbital of the aromatic system (see below in Molecular Orbital Calculations). Such transitions are shifted to very high energies since the nitrogen nonbonding orbitals become bonding upon coordination to the metal, thus increasing the difference between the energies of the π^* and the energies of the former n orbitals.

Molecular Orbitals Calculations. DFT calculations[34] using the ADF program[35] were performed for the ligands **IIa** and **IIb**, and for the two complexes **2a** and **2b**. The geometries were fully optimized, and the agreement between the calculated distances (see below) and angles for **IIb** and **2b** with the corresponding values obtained from

(49) Su, Q.; Gao, W.; Wu, Q.-L.; Ye, L.; Li, G.-H.; Mu, Y. *Eur. J. Inorg. Chem.* **2007**, 4268–4175.
(50) (a) Yang, W.; Schmider, H.; Wu, Q.; Zhang, Y.-S.; Wang, S. *Inorg. Chem.* **2000**, *39*, 2397–2404. (b) Wu, Q.; Lavigne, J. A.; Tao, Y.; D'Iorio, M.; Wang, S. *Inorg. Chem.* **2000**, *39*, 5248–5254.
(51) Ghedini, M.; La Deda, M.; Aiello, I.; Grisolia, A. *J. Chem. Soc., Dalton Trans.* **2002**, 3406–3409.

Table 4. Composition, Energy (eV), Calculated and Experimental Absorption Wavelengths (nm), and Oscillator Strength (OS) of the More Relevant Electronic Transitions of Ligand Precursors **IIa** and **IIb** and of Zn Complexes **2a** and **2b**

no.	composition	energy (eV)	wavelength (nm)	λ_{exp}[a] (nm)	OS
	Ligand Precursor **IIa**				
1	H-1→L (58%); H→L (28%)	3.017	411	383	0.097
2	H-1→L (35%); H→L (28%); H→L+1 (14%); H-2→L (10%); H-3→L (8%)	3.118	398		0.051
3	H-2→L (44%); H-3→L (25%); H→L+1 (14%); H→L (11%)	3.229	384		0.071
4	H-3→L (43%); H→L (19%); H-2→L (12%); H-1→L+1 (12%)	3.565	348		0.207
	Ligand Precursor **IIb**				
1	H-1→L (54%); H→L (45%)	2.751	450	369	0.031
2	H→L+1 (38%); H→L (19%); H-1→L (16%); H-2→L (15%)	3.110	399		0.070
3	H→L+1 (43%); H-1→L+1 (21%); H-1→L (13%); H→L (12%)	3.170	391		0.078
4	H-2→L (52%); H-4→L (22%); H-1→L+1 (12%)	3.240	383		0.068
5	H→L+2 (39%); H-1→L+2 (33%); H-4→L (15%)	3.544	350		0.048
6	H-4→L (37%); H-1→L+2 (17%); H-2→L (12%); H→L+2 (10%)	3.554	349		0.185
	Complex **2a**				
1	H-1→L+1 (22%); H-3→L+1 (18%); H-2→L (18%); H→L (17%);	2.857	434	448	0.166
2	H-3→L (20%); H-2→L+1 (14%); H→L+1 (14%); H-5→L (14%); H→L (14%)	2.907	426		0.409
3	H-3→L+1 (23%); H-1→L+1 (16%); H-5→L+1 (14%); H-2→L (14%)	2.934	423		0.214
4	H-5→L (35%); H-4→L+1 (28%); H-1→L+2 (8%)	3.153	393		0.190
5	H-5→L+1 (30%); H→L+2 (21%); H-4→L (16%)	3.164	392		0.183
6	H→L+2 (39%); H-1→L+3 (30%)	3.176	390		0.101
	Complex **2b**				
1	H→L+1 (54%); H-2→L+1 (17%)	2.795	444	405	0.220
2	H-1→L (45%); H-2→L (17%); H-1→L+1 (11%)	2.805	442		0.172
3	H-3→L (30%); H-2→L+1 (26%); H-3→L+1 (11%); H→L+1 (10%)	2.900	428		0.259
4	H-1→L+2 (47%); H-5→L (31%)	3.151	393		0.032
5	H-4→L+1 (39%); H-1→L+2 (14%); H-5→L (14%)	3.156	393		0.084
6	H-5→L (23%); H-1→L+2 (22%); H-5→L+1 (20%)	3.172	391		0.032

[a] From Table 3.

single crystal X-ray diffraction studies (see above) is very good. Therefore it is expected that the structures calculated for **IIa** and **2a** will be reliable.

TD-DFT calculations[41] were performed on the four molecules to calculate the nature and energy of the lowest energy transitions. The results, namely, the energy, wavelength, and oscillator strength of the more intense bands, are collected in Table 4.

There are two groups of bands, the first closer to 400 nm, defining the absorption maximum, and the second which appears as a shoulder at higher energy. The shift to lower energies of the absorption maxima upon moving from the ligand precursors **IIa** and **IIb** to the complexes of the deprotonated ligands **2a** and **2b** is well reproduced. It is not so easy to see the effect of the isopropyl substituents, as a global maximum can be adjusted when simulating the spectra, but the trends are kept. The calculated maxima for complexes **2a** and **2b** can be found at 433 and 422 nm, not too far from the experimental 448 and 405 nm.

In the smaller ligand **IIa**, the transitions are mixed, starting from H-3, H-2, H-1, and H, and ending in L and L+1. The nitrogen atom attached to the phenyl ring contributes to the four occupied orbitals, but while H and H-2 are completely π systems, the nitrogen lone pair has a strong contribution to H-1 and a much smaller in H-2. Therefore, the transitions can be assigned as a combination of $n\rightarrow\pi^*$, $\pi\rightarrow\pi^*$, and intraligand (IL) $\pi\rightarrow\pi^*$, as can be seen in Figure 4. The compositions of the orbitals of the ligands **IIa** and **IIb** are given in Supporting Information, Table S3.

From a qualitative point of view the orbitals involved in the transitions of ligand **IIb** are very similar to those described above (see Supporting Information, Figure S5). The transitions start from H-4, H-2, H-1, and H, and end in L, L+1, and L+2. In terms of composition, the nitrogen lone pair only contributes to H-1. H-4 of **IIb** is the analogue of H-3 in **IIa** and localized in the phenyl ring, but with some contribution from the isopropyl groups in **IIb**. On the other hand, two unoccupied orbitals (L and L+2) are strongly localized in the imine C=N π bond, while the major contribution to L+1 are the benzene rings of the phenanthrene fragment (see Supporting Information, Figure S5). The energies of the orbitals of the ligand precursor **IIb** are higher than those of **IIa**.

The nature of the orbitals changes when the ligand precursors lose a proton and bind the metal, since the nitrogen σ lone pairs (now also a second one on the pyrrolyl group) are involved in Zn−N σ bonds and therefore they no longer belong to the group of frontier orbitals. In the complexes, the frontier orbitals are mostly localized in the ligands, since the d^{10} Zn based levels are all filled and have lower energies, as can be seen in the Supporting Information, Table S4. The orbitals come in pairs, corresponding to the symmetric and antisymmetric combinations of a given orbital of each ligand, or localized in each of them. L+2 and L+3 of **2a** are almost totally localized in the phenanthrene of one ligand in L+2 and in the phenanthrene of other ligand in L+3, and have almost the same energy. L and L+1 are more delocalized over the two ligands. The energy of the frontier orbitals of the complexes are close to those of the ligand precursors,

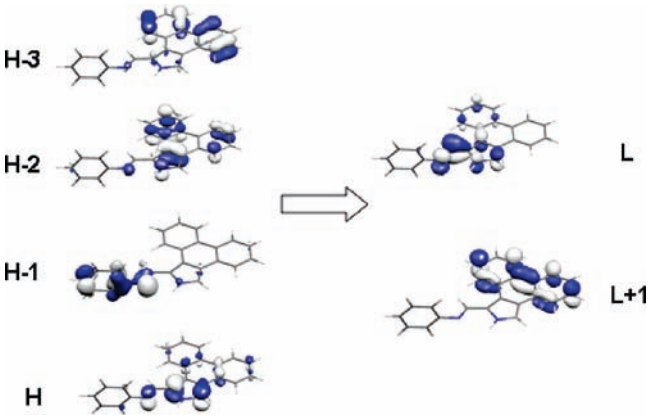

Figure 4. Orbitals involved in the stronger absorptions of ligand precursor **IIa**.

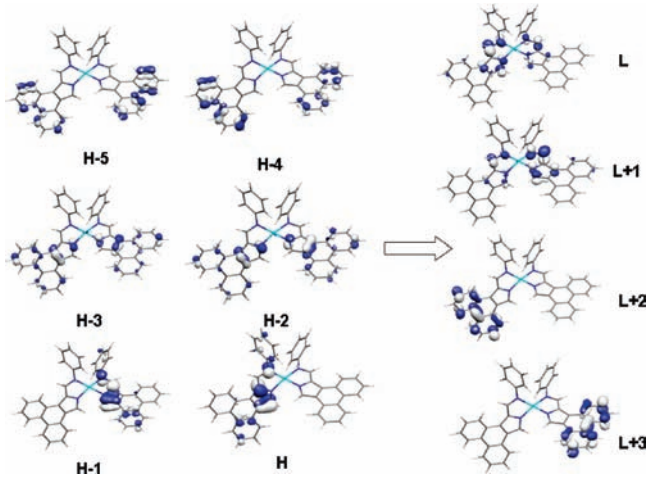

Figure 5. Orbitals involved in the stronger absorptions of complex **2a**.

as might be expected, since they are essentially π orbitals, only very weakly involved in binding the metal.

In terms of transitions, the oscillator strengths are larger in the complexes than in the ligand precursors, while the transitions involve only π and π^* orbitals of the ligands. The orbitals involved in the electronic transitions of complex **2a** are shown in Figure 5 and show a complete localization on the π systems, either belonging to the phenyl, to the phenanthrene, or the N−CH−C−N regions.

These calculations were also performed taking into account the solvent (THF), but there were no significant differences from the behavior in gas-phase.

To study the emission of the molecules, the geometry of the first singlet excited state was optimized, promoting one electron to the LUMO. Some relevant structural parameters of the ground and excited state are given in Supporting Information, Figure S7.

The excitation of one electron leads to changes in several bond lengths, namely, the shortening of the NC−CN bond, and lengthening of the C−N bonds, in both ligands. The angle between the two rings, measured by the C−N−C−C torsion, changes from 76.1°, in the ground state of **IIa**, to 21.2°, in the singlet excited state. The change is less pronounced in ligand precursor **IIb** (from 79.9° to 51.8°), reflecting the steric hindrance of the isopropyl substituents.

Table 5. Emission Energy (eV) and Wavelength (nm) from the First Excited Singlet State of Ligand Precursors **IIa** and **IIb**, and the Complexes **2a** and **2b**, in the Gas Phase and in THF

	gas phase		THF	
compound	E_{gp}	wavelength	E_{THF}	wavelength
IIa	1.792	693	1.814	684
IIb	1.879	660	1.922	645
2a	1.822	681	1.853	669
2b	1.965	631	1.978	626

The comparison between the first and third row pictures of Supporting Information, Figure S7 shows the effect of coordinating ligand precursor **IIa** after deprotonation to Zn to afford **2a**. The asymmetry between the two halves of the molecule results from the promotion of one electron to the LUMO, differently localized in the two sides (recall the nature of the frontier orbitals discussed above). The effect is clearly seen on the right side of the molecule (shortening of the NC−CN bond, lengthening of the C−N bonds, similar torsion angle).

Because configuration interaction is computationally very demanding and not easily carried out, especially for large molecules as complexes **2a** and **2b**, the emission energy (E_{gp}) was estimated as the difference between the energy of this singlet excited state and the energy of a ground state with the same geometry (gas phase), and is listed in Table 5. The calculations were repeated in the presence of the solvent (THF; details in Experimental Section) and another energy (E_{THF}) was calculated.

Not surprisingly, the results do not agree with the experimental values (Table 3), and the solvent effect is negligible. However, the trend within each group (ligand precursors or complexes) is kept, with lower emission wavelengths in the compounds bearing the isopropyl substituents.

Conclusions

The synthesis and molecular characterization of new homoleptic Zn(II) complexes containing aryliminophenantzhro[9,10-*c*]pyrrolyl ligands was achieved in moderate to very high yields. We have measured the photophysical properties of both ligand precursors and complexes and compared them with those of analogues containing simple iminopyrrolyl ligands. The fluorescence spectra of the metal complexes show much more intense $\pi-\pi^*$ fluorescence emissions than those of the free ligand precursors, which are partially forbidden because of their $n-\pi^*$ character. The great enhancement in the fluorescence quantum yields observed upon deprotonation and coordination of the iminophenanthropyrrolyl ligands to the d^{10} spectroscopically inactive Zn^{2+} ion is due to their highly resonant π-extended conjugation and to the use of the nitrogens non-bonding electrons in the σ-coordination to the metal. The DFT calculations confirmed the role of $n-\pi^*$ transitions in the electronic spectra of the ligand precursors and their absence in the complexes. Complex **2a** is a green emitter and presents the highest fluorescence quantum yield. The bulkiness of the 2,6-diisopropylphenyl substituent of the iminic group highly restricts the aryl group rotation, inducing a shift in the emission to the blue region. In summary, the new aryliminophenanthro[9,10-*c*]pyrrolyl framework exhibits very interesting luminescent properties and tuning capabilities when coordinated to Zn^{2+}

ions. The results herein obtained anticipate the possibility of improvement of the luminescence properties of this type of complexes by further chemical modifications of the ligand framework and/or by varying the metal. Studies aiming at the use of these compounds in light emitting devices or as sensors are in progress.

Acknowledgment. The authors thank the *Fundação para a Ciência e Tecnologia*, Portugal, for financial support (Projects PTDC/QUI/65474, PPCDT/QUI/59025/2004, and PPCDT/QUI/58925/2004, co-financed by FEDER) and for fellowships to C.S.B.G. (SFRH/BD/16807/2004) and R.E.D.P. (SFRH/BPD/34558/2007), and the Portuguese NMR Network (IST-UTL Center) for providing access to the NMR facility.

Supporting Information Available: CIF files containing X-ray structural data, including data collection parameters, positional and thermal parameters, and bond distances and angles, for compounds **IIb** and **2b**; syntheses of 2-formiminopyrrole ligand precursors **Ia**,**b** and corresponding analytical data; schemes containing the multistep preparation of 2-formylphenanthro-[9,10-*c*]pyrrole (Scheme S1 and S2); X-ray molecular structure of complex **2b** (Figure S1) and its discussion, and corresponding table with selected bond distances and angles (Table S1); absorption and emission spectra of ligand precursors **Ia**,**b** and complexes **1a**,**b** (Figure S2); photophysical parameters of complexes **1a** and **1b** and their corresponding neutral ligand precursors **Ia** and **Ib** (Table S2); fluorescence decays of ligand precursors **IIa**,**b** (Figure S3) and of complexes **2a**,**b** (Figure S4); orbitals involved in the stronger absorptions of ligand precursor **IIb** (Figure S5) and complex **2b** (Figure S6); energy and composition of the frontier orbitals of ligand precursors **IIa**,**b** (Table S3) and complexes **2a**,**b** (Table S4); optimized geometries of the ground and first excited singlet states of ligand precursors **IIa**,**b** and complexes **2a**,**b** (Figure S7). This material is available free of charge via the Internet at http://pubs.acs.org.